forests

MDPI

Article

Spatial Partitioning and Driving Factors of Soil Carbon and Nitrogen Contents in Subtropical Urban Forests—A Case of Shenzhen, China

Zhiqiang Dong [1,2,3,4], Shaobo Du [1], Xufeng Mao [1], Huichun Xie [2,3,4,5,6,*], Zhengjun Shi [7,8,*] and Wei Zeng [7,8]

1 College of Geographical Sciences, Qinghai Normal University, Xining 810008, China
2 Qilian Mountain Southern Slope Forest Ecosystem Research Station, Haidong 810500, China
3 Key Laboratory of Medicinal Animal and Plant Resources of Qinghai-Tibetan Plateau, Xining 810008, China
4 Team of Germplasm Resources Formation Mechanism and Utilization on the Qinghai-Tibetan Plateau, Xining 810008, China
5 School of Life Sciences, Qinghai Normal University, Xining 810008, China
6 Innovation and Intelligence Introduction Base for Plateau Resources Ecology and Sustainable Development, Xining 810008, China
7 Key Laboratory of Southern Subtropical Plant Diversity, Fairylake Botanical Garden, Shenzhen & Chinese Academy of Sciences, Shenzhen 518004, China
8 China Shenzhen Urban Forest Ecosystem Research Station, State Administration of Forest and Grassland, Shenzhen 518004, China
* Correspondence: yezino.1@163.com (H.X.); shizhengjun@szbg.ac.cn (Z.S.); Tel.: +86-136-3978-6226 (H.X.); +86-135-3069-9756 (Z.S.)

Abstract

Global change seriously affects human survival, and urban forests can improve human living environments and mitigate the negative impacts of global change. The spatial distribution of carbon and nitrogen is key to assessing the health of forest ecosystems. However, the mechanism underlying the spatial distribution of carbon and nitrogen in urban forests in subtropical regions remains unclear. To study the characteristics and factors influencing the carbon and nitrogen contents of forest soils in Shenzhen, 126 soil samples were collected. Multivariate statistics and spatial analysis methods revealed the spatial distribution patterns and influencing factors of SOC, TN, and C/N in Shenzhen forest soils. The results showed the following: (1) The mean values of SOC, TN, and C/N of the 0–10 cm soil were 18.32 $g \cdot kg^{-1}$, 1.29 $g \cdot kg^{-1}$ and 14.43, with coefficients of variation (CVs) of 38.21%, 37.98%, and 15.73%, respectively, and those of the 10–30 cm soil were 9.24 $g \cdot kg^{-1}$, 0.67 $g \cdot kg^{-1}$, and 13.75, with CVs of 45.24%, 41.79%, and 19.45%, respectively. (2) The kriging spatial interpolation showed that the high- and low-value areas of 0–10 cm SOC and TN were concentrated in the northwestern and central and northern parts of the study area, respectively. The high value areas of 10–30 cm SOC and TN expanded to the southeastern part of the study area, and the low-value areas of SOC were distributed in the northern part. (3) The edges of the study area were fragmented, and the low-value areas of TN were mainly distributed in the western region, the high-value areas of C/N were mainly distributed in the west, and the low-value areas were mainly distributed at the eastern edge. Soil bulk weight and conductivity were the key factors affecting SOC and TN, which were the key factors affecting C/N. We emphasized the inhomogeneity of the spatial distribution of C/N in the subtropical region and that soil C/N is co-regulated by multiple factors. The results may provide insights for the government's urban green space construction.

Keywords: forest soil; urbanization; soil bulk density; urban green space

check for updates

Received: 13 August 2025
Revised: 15 September 2025
Accepted: 18 September 2025
Published: 19 September 2025

Citation: Dong, Z.; Du, S.; Mao, X.; Xie, H.; Shi, Z.; Zeng, W. Spatial Partitioning and Driving Factors of Soil Carbon and Nitrogen Contents in Subtropical Urban Forests—A Case of Shenzhen, China. *Forests* **2025**, *16*, 1492. https://doi.org/10.3390/f16091492

Copyright: © 2025 by the authors. Licensee MDPI, Basel, Switzerland. This article is an open access article distributed under the terms and conditions of the Creative Commons Attribution (CC BY) license (https://creativecommons.org/licenses/by/4.0/).

1. Introduction

In the context of increasing global change, urbanization, as a central driver, is profoundly reshaping soil ecosystems and exacerbating their challenges. Since the twentieth century, soil ecosystems have faced enormous challenges as a result of rapid urbanization and industrialization [1,2]. Soil compaction leads to reduced aeration, affecting microbial activity and nutrient transformation [3]. Infiltration of pollutants from industrial wastewater, exhaust gases, and municipal waste into the soil [4] causes excessive heavy metal and organic matter contamination of soil [5]. Large amounts of forested and cultivated land have been encroached upon in urban sprawl, and soil carbon pools have been reduced in storage and stability [6]. Anthropogenic disturbances change the original vegetation cover of the soil, reducing the input of apoplastic material, which in turn affects the accumulation and cycling process of soil carbon and nitrogen content [7]. Urban forest soils are essential for enhancing the sustainability of urban environments; maintaining the ecological balance of soils, plants, microorganisms, microbial activity, and decomposition of organic matter [8]; and promoting harmony between humans and nature [9].

In recent decades, the characterization of the spatial variability of soil organic carbon and total nitrogen has been a topic of great interest in the field of soil ecology [10–12], mainly in natural ecosystems with low anthropogenic intervention, such as farmlands [13], grasslands [14], and forests [15]. There are fewer studies on the spatial variability of soil carbon and nitrogen content and the driving mechanisms in urbanized areas, and the studies on urban soils have mainly focused on the comparison of SOC and TN and spatial distribution of SOC and TN under different land-use modes [16,17]. Soil organic carbon is a core pool in the terrestrial carbon cycle, and soil total nitrogen is a key limiting nutrient for plant growth; in subtropical urban forests under the context of urbanization, the spatial distribution and dynamic balance of these two components are susceptible to changes caused by anthropogenic disturbances, which directly affect the functions of forest ecosystems [18].The soil carbon-to-nitrogen ratio is a key indicator of organic matter decomposition rate; in subtropical urban forest soils, C/N typically decreases with increasing soil depth and is regulated by the quality of vegetation litter and microbial activity. Abnormal changes in C/N can reflect the impact of anthropogenic disturbances on soil organic matter cycling. Soil carbon and nitrogen form a close coupled relationship mediated by microorganisms, SOC provides energy for microorganisms to drive nitrogen mineralization, while the availability of TN limits vegetation carbon input [19]. This interaction is more likely to be disrupted by anthropogenic disturbances in highly urbanized regions such as Shenzhen. Few studies have examined the spatial distribution and driving mechanisms of soil C/N in highly urbanized forests. In highly urbanized areas, vegetation, soil, topography, and climatic and anthropogenic factors affect soil C/N content. GDP, population density, nighttime light index, and distance to municipal centers can reflect the intensity of anthropogenic disturbances [20]. However, it is unclear how these factors affect soil carbon and nitrogen content and C/N in urban forests.

Previous studies have extensively investigated the spatial variability of its nutrients using methods such as geostatistics and semi-variogram functions [21–23], However, traditional statistical methods or single-scale sampling strategies have difficulty in accurately revealing the spatial variation of carbon and nitrogen from small to regional scales under complex topography and land-use patterns. In this study, the spatial patterns of carbon and nitrogen in forest soils in Shenzhen were analyzed using multivariate and geostatistics. In the study of spatial variability of soil carbon and nitrogen, Redundancy Analysis serves as a key method to address the limitation that traditional single-factor statistics struggle to distinguish the synergistic effects of multiple factors. This is because it can integrate multiple types of explanatory variables, quantitatively analyze their contribution to the variation

in response variables (SOC, TN, C/N), and intuitively present the relationships between factors via ordination diagrams. Notably, it is particularly suitable for studying the driving mechanisms of soil indicators in the complex environment of urbanized areas [24]. In this study, 126 soil samples were collected from forest soils (0–10 cm and 10–30 cm) in Shenzhen, and the spatial distribution of carbon and nitrogen content and C/N in the 0–30 cm soil layer were investigated by combining field investigations and laboratory analyses. The objectives of this study were (1) to reveal the spatial distribution characteristics of SOC, TN, and C/N; (2) to quantify the contributions of climate, geomorphology, vegetation, and soil physicochemical and anthropogenic factors to their spatial variability; and (3) to determine the strength of the coupled effects and pathways of natural and anthropogenic factors on the spatial heterogeneity of soil carbon and nitrogen in different soil layers. This study provides a region-specific scientific basis for analyzing the carbon and nitrogen cycling mechanisms of forest soils in urbanized areas.

2. Materials and Methods

2.1. Overview of the Study Area

Shenzhen is located in the southern coast of Guangdong Province, south of the Tropic of Cancer, longitude 113°45′44″ E–114°37′21″ E, latitude 22°26′59″ N–22°39′21″ N, with a land area of 1997.45 km^2 and a subtropical oceanic climate. The landforms are diversified, mainly low hills, followed by terraces and coastal plains, and the highest peak in the territory is Wutong Mountain, with an elevation of 944 m. The overall elevation distribution of the study area and the spatial scope involved in this research are visualized in Figure 1. There are 10 soil classes and 15 subclasses, mainly reddish loam, yellow loam, reddish loam, and coastal sandy loam, and the parent materials of the soil-forming materials are mainly granite and sandy shale. Reddish loam is distributed in hilly mountains and slopes below 300 m above sea level, reddish loam is mainly distributed in the middle and upper parts of mountains at an altitude of 300–600 m, and yellow loam is mainly distributed in the middle and upper parts of low mountains above 600 m. The average temperature of Shenzhen is 22.5 °C, with abundant rainfall and an average annual rainfall of 1932.9 mm. The zonal vegetation is coastal-type evergreen broad-leaved forests in the southern subtropical monsoon, and the existing major forest vegetation includes *Cinnamomum camphora*, *Dimocarpus longan*, *Litsea rotundifolia*, *Castanopsis fissa*, *Liquidambar formosana* and *Syzygium cumini*.

2.2. Soil Sampling and Determination of Indicators

According to the topographic map of the study area and the distribution characteristics of vegetation types, the study area was scientifically distributed, and 126 soil samples were collected in the field (soil depths of 0–10 cm and 10–30 cm). The field coordinates, elevation, vegetation types, and other information of the sampling points were recorded using a GPS. The air-dried in situ soil samples were pulverized and soil pH, EC were determined by passing them through a 1 mm sieve, and SOC, TN were determined by passing them through a 0.25 mm sieve. Soil pH was determined in a ratio of soil to liquid of 1:2.5 (*v*/*v*) by a compound electrode (PE-10; Sartorious, Germany). Soil EC was determined by conductivity meter with a suspension ratio of soil to distilled water of 1:5 (DDS-11A, Shanghai Leici Xinjing Instrument Co., Ltd., Shanghai, China). The concentrated sulfuric acid-potassium dichromate method was used to measure soil OC content. After digestion of the soil with sulfuric acid, soil TN was determined by soil TN was determined using the semi-micro-Kjeldahl nitrogen determination method. The particle size distribution of aggregates was determined using the dry sieving method. For each measurement, 250 g of air-dried soil sample was weighed and placed on the top layer of nested sieves, with aperture sizes of 10 mm, 5 mm, 3 mm, 2 mm, 1 mm, 0.5 mm, and 0.25 mm in sequence. The

nested sieves were placed on a sieve shaker and oscillated for 10 min, after which the soil retained on each sieve was weighed. Given that excessively fine initial classification might obscure key ecological associations, the aggregates were ultimately merged into 3 functional classes through Pearson correlation analysis between each particle size fraction and soil organic carbon, total nitrogen, and carbon-to-nitrogen ratio: >1 mm (macroaggregates), 0.25–1 mm (mesoaggregates), and <0.25 mm (microaggregates). The mean weight diameter (MWD) and geometric weight diameter (GWD) were calculated based on the mass of aggregates measured via the dry sieving method.

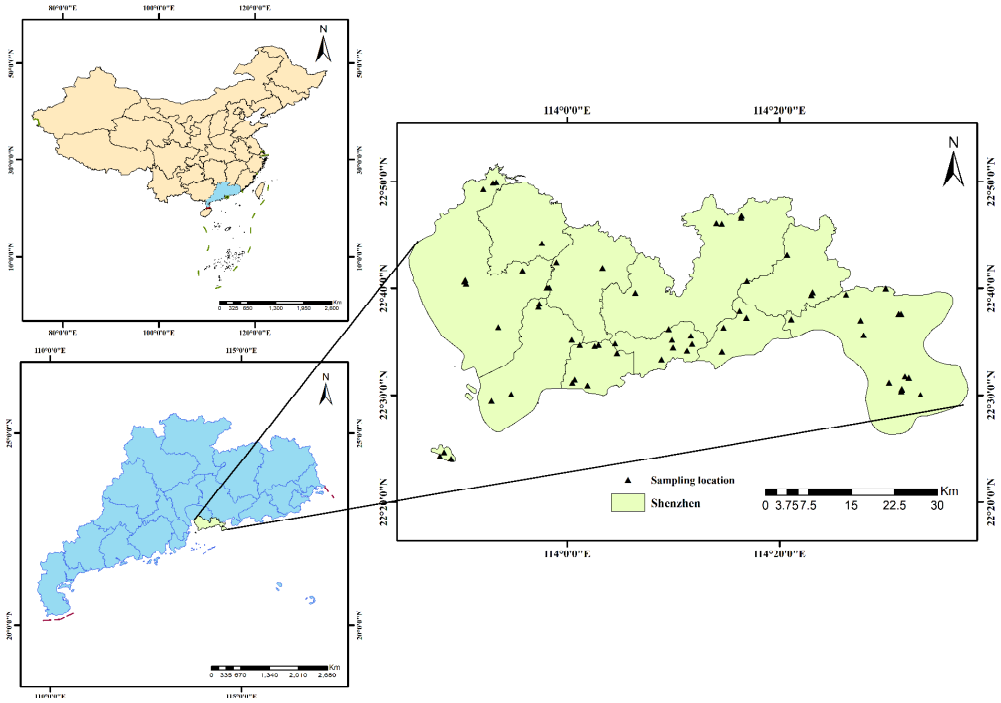

Figure 1. Sample distribution and elevation maps of the study area in Shenzhen City, China.

2.3. Driver Data Acquisition

Factors included climatic (mean annual temperature and rainfall, all data are sourced from the National Earth System Science Data Center), geomorphic (elevation and slope), soil physicochemical (pH, conductivity, soil bulk weight, force-stabilizing aggregates, MWD, and GWD), anthropogenic (GDP, population density, nighttime light index, and distance from municipal government. Nighttime Light Index data is sourced from the Resource and Environmental Sciences Data Center, and it refers to nighttime light data acquired by the NPP-VIIRS satellite. GDP and population density data are sourced from the National Tibetan Plateau Scientific Data Center, which are gridded spatial distribution datasets obtained by spatially matching the statistical GDP values of administrative units with nighttime light index data. Distance to City Hall was calculated using the Proximity Analysis tool in ArcGIS, based on the vector points of Shenzhen municipal government locations and the study area boundary data provided by the National Geomatics Center of China), and vegetation (normalized vegetation index, vegetation cover, vegetation primary productivity, degree of depression, and average tree height. The Normalized Difference Vegetation Index (NDVI) data is sourced from the Resource and Environmental Sciences Data Center, specifically the annual maximum composite NDVI data derived from the Landsat-8 satellite. The Net Primary Productivity (NPP) data is also obtained from the Resource and Environmental Sciences Data Center, generated via simulation using the CASA (Carnegie-Ames-Stanford Approach) model. Vegetation Coverage is retrieved from NDVI data using the "pixel dichotomy method". The anthropogenic factors directly reflect

the urbanization process, which determines the demand for land development; the climatic factors indirectly regulate the land-use mode by influencing the regional hydrological cycle; the geomorphic factors constrain the spatial distribution of construction activities; and the vegetation factors, particularly the Normalized Difference Vegetation Index (NDVI) and Net Primary Productivity, reflect the blocking effect of the ecological substrate on the expansion of the city, and the dynamics of their changes are often significantly negatively correlated with the urbanization process. Dynamic changes in these factors often show a significant negative correlation with urbanization. The combination of these five driving factors can reveal the mechanisms of human-led expansion and identify the regulatory roles of natural systems (Table 1).

Table 1. Environmental variables and their data sources in Shenzhen City, China (for analyzing driving factors of soil SOC, TN, and C/N in subtropical urban forests).

Driving Factor	Type	Units	Resolution	Data Sources
Climatic	Average annual temperature	°C	1 km	National Earth System Science Data Center
	Average annual rainfall	mm	1 km	National Earth System Science Data Center
Geomorphologic	Elevation	m	/	Real time data
	Slope	°	/	Real time data
Human	Nighttime Lighting Index	/	/	Resource and Environmental Sciences Data Center
	GDP	CNY·km^{-2}	1 km	National Tibetan Plateau Data Center
	Population density	persons·km^{-2}	/	Oak Ridge National Laboratory, USA
	Distance to City Hall	m	/	National Center for Basic Geographic Information
Plant	Normalized Difference Vegetation Index	/	1 km	Resource and Environmental Sciences Data Center
	Fractional Vegetation Cover	%	250 m	Resource and Environmental Sciences Data Center
	Net Primary Productivity	g/(m^2·a)	1 km	Resource and Environmental Sciences Data Center
Soil	Crown density	/	/	Real time data
	Average tree height	m	/	Real time data
	pH	/	/	Real time data
	Conductivity	dS/cm	/	Real time data
	Bulk density	g/cm^3	/	Real time data
	Mechanical stable aggregate	mm	/	Real time data
	Mean weight diameter	mm	/	Real time data
	Geometric mean diameter	mm	/	Real time data

2.4. Data Processing

In this study, SPSS 27.0 software was used to process the data for outliers, and the data were tested according to the mean ± 3 times the standard deviation and after detecting and removing the outliers, followed by descriptive statistics and normal distribution test, and the normality of the dataset was tested by the Kolmogorov–Smirnov test (K–S), with $p > 0.05$, indicating that the data conforms to a normal distribution. If the data did not conform to a normal distribution, the data were logarithmically transformed. Pearson correlation analysis was used to study the correlation between SOC, TN, and C/N and

other quantitative indicators; One way analysis of variance (ANOVA) was adopted to examine differences in SOC, TN, and C/N across vegetation types, and the Duncan's new multiple range test was then applied when significant differences were detected by the ANOVA. Pearson correlation analysis was used to study the correlation between SOC, TN, and C/N and other quantitative indicators; descriptive statistics were performed on SOC, TN, and C/N indicators, and their average conditions and degree of variation were analyzed by standard deviation and coefficient of variation (CV), and the CV < 10%, 10%–100%, and >100% belonged to low, medium, and high intensity variations, respectively. The spatial autocorrelation coefficients were calculated and spatial distribution maps were plotted using ArcMap 10.8 software; the semivariate variance function analysis was performed using GS+ 9.0 software; the correlation analysis and plotting were performed using Origin 2021 software; the redundancy analysis was plotted using CANOCO 5.0; and the redundancy analysis maps were plotted using the R packages "relaimpo" and "ggplot2" in the R 4.2.1 software. "Relaimpo" [25] and "ggplot2" [26] in R 4.2.1 software were used to calculate and plot the variance decomposition analysis; partial least squares structural equation modeling was calculated using the R package "plspm" [27].

3. Results

3.1. Descriptive Analysis of SOC, TN, and C/N

The descriptive statistical results of soil organic carbon (SOC), total nitrogen (TN), and carbon-to-nitrogen ratio (C/N) clearly demonstrate the vertical stratification characteristics and spatial variability of carbon and nitrogen in the forest soils of Shenzhen. Table 2 shows that the SOC, TN, and C/N contents of the 0–10 cm soil in this study area ranged from 3.18 to 33.81 g·kg^{-1}, 0.26 to 2.41 g·kg^{-1}, and 7.7 to 19.29, with mean values of 18.32 g·kg^{-1}, 1.29 g·kg^{-1}, and 14.43, respectively. The SOC, TN, and C/N contents of the 10–30 cm soil ranged from 1.3 to 23.68 g·kg^{-1}, 0.18 to 1.33 g·kg^{-1}, and 7.7 to 19.29, with mean values of 9.24 g·kg^{-1} and 14.43, respectively. C/N ranged from 1.3 to 23.68 g·kg^{-1}, 0.18 to 1.33 g·kg^{-1}, and 7.7 to 19.29, with mean values of 9.24 g·kg^{-1}, 0.67 g·kg^{-1}, and 13.75, respectively. The CVs reflected the degree of dispersion of SOC, TN, and C/N, and the SOC, TN, and C/N in this study area were all <50%. The CVs were 38.21%, 37.98%, and 15.73% for the 0–10 cm soil, and 45.24%, 41.79%, and 19.49% for the 10–30 cm soil, respectively, which were at the medium level of variability, indicating that the spatial distributions of SOC, TN, and C/N were not homogeneous. which reflects that the carbon and nitrogen accumulation effect driven by recent vegetation litter input is more pronounced in the surface soil layer. Meanwhile, the coefficients of variation of both soil layers are at a moderate level, indicating that the carbon and nitrogen distribution is jointly regulated by natural topography and anthropogenic disturbances. Furthermore, the subsoil, affected by structural factors such as parent material differences, exhibits a slightly higher degree of variation than the surface soil layer. The results of the normality test of the K–S method showed that the SOC, TN, and C/N conformed to a normal distribution.

3.2. Characterization of the Spatial Distribution of SOC, TN, and C/N

The theoretical fitting models for SOC, TN, and C/N were analyzed using geostatistical semi-variance characteristic parameter functions (Table 3). The distribution models for SOC and TN differed at different soil depths. The 0–10 cm SOC conformed to the spherical model, TN conformed to the Gaussian model, 10–30 cm SOC conformed to the Gaussian model, TN conformed to the exponential model, and the soil C/N conformed to the linear model. The fitted models accurately reflected the spatial variability of SOC, TN, and C/N in Shenzhen forest soils. The block base ratio is an important parameter for the degree of spatial variability of regionalized variables, which can measure the degree of spatial

dependence of the indicators. The range of variability responds to the spatial continuity of the indicators at the regional scale. In the soil, the SOC and TN block ratios were <25%, showing high spatial autocorrelation, indicating that the spatial variability was mainly affected by structural factors (parent material, topography and other natural conditions); the soil C/N block ratios were >75%, showing weak spatial autocorrelation, suggesting that the variability was mainly affected by stochastic factors. TN and C/N were 6948.99 m, 21,330 m, and 12,380.85 m, respectively, indicating that environmental factors affected the spatial heterogeneity of SOC in a small range. Cross-validation results indicated that the 0–10 cm topsoil exhibited lower MAPE values for SOC, TN, and C/N; however, the RMSE values of SOC and TN in this topsoil layer were higher than those in the 10–30 cm subsurface soil. This phenomenon may be attributed to the significant anthropogenic disturbances affecting the topsoil, which ultimately led to its higher RMSE compared to the subsurface layer.

Table 2. Descriptive statistics of key indicators (SOC, TN, C/N) in 0–10 cm and 10–30 cm forest soils of Shenzhen City, China.

Index	Depth (cm)	Min/(g·kg^{-1})	Max/(g·kg^{-1})	Average Value/(g·kg^{-1})	Standard Deviation	Coefficient of Variation (%)	Skewness	Kurtosis	$p_{(K-S)}$
SOC	0–10	3.18	33.81	18.32	7.00	38.21	0.07	−0.36	0.20
	10–30	1.30	23.68	9.24	4.18	45.24	0.87	1.33	0.20
TN	0–10	0.26	2.41	1.29	0.49	37.98	0.02	−0.32	0.20
	10–30	0.18	1.33	0.67	0.28	41.79	0.35	−0.52	0.20
C/N	0–10	7.70	19.29	14.43	2.27	15.73	0.01	0.01	0.20
	10–30	5.29	20.44	13.75	2.68	19.49	−0.07	1.41	0.05

Table 3. Theoretical model of the ratio of SOC, TN, and C/N in the study area and its related parameters.

Index	Depth (cm)	Theoretical Model	Nugget Value	Abutment Value	Block Base Ratio/%	Range/m	R^2	I_N	Z	Cross Validation	
										MAPE	RMSE
SOC	0–10	Spherical	6.6	74.8	8.82	2443	0.39	0.62	13.35	0.24	4.96
	10–30	Gaussian	0.22	3.45	6.38	6948.99	0.49	0.25	5.48	0.36	4.07
TN	0–10	Gaussian	0	0.33	0.3	864.29	0.54	0.47	10.58	0.28	0.54
	10–30	Exponential	0.03	0.37	7.22	21,330	0.31	0.22	4.92	0.31	0.33
C/N	0–10	Linear	4.05	4.05	100	11,031.57	0.78	0.42	8.99	0.14	2.14
	10–30	Linear	7.23	7.23	100	12,380.85	0.63	0.29	6.38	0.31	3.14

3.3. Spatial Autocorrelation Analysis of Soil Nutrients

The global Moran's *I* index can more intuitively reflect the aggregation status of soil attributes in the entire study area, standardize the data in the random condition, use the confidence interval two-sided test threshold as the boundaries, and statistically test the significance of the indicator spatial autocorrelation. The larger the absolute value, the more evident the spatial autocorrelation. The SOC, TN, and C/N results analysis for forest soil soils in Shenzhen City (Table 2) showed that SOC, TN, and C/N had significant spatial autocorrelation ($p < 0.001$, $|Z| \geq 2.58$). The local Moran's *I* index (Figure 2) was calculated by spatially connecting the mean values of the interpolated results within the townships to the evaluation unit, and the local Moran's *I* index was calculated to form the LISA clustering map. The 0–10 cm SOC high-value clusters were mainly distributed in the northwest, and low-value clusters were mainly distributed in the north and south, with a small part of the high–low anomaly area. TN high-value clusters were mainly distributed in the north and south of the soil. High-value TN aggregation areas were mainly distributed in the northwest, low-value aggregation areas were mainly distributed in the north and south, and there were high–low anomalies around the low-value aggregation areas in the

south, with a few low–high aggregation areas in the south of the high-value aggregation areas. High-value C/N aggregation areas were distributed in the west and northeast, low-value aggregation areas were distributed in the northwest and south, and there were a few high–low aggregation areas in the southern low-value aggregation areas. The 10–30 cm SOC high-value aggregation area is mainly distributed in the northwest and central areas, the low-value aggregation area distribution was more dispersed, with broken distribution, and accompanied by a small part of the low–high, high–low aggregation area. The TN and SOC distribution was similar, the high-value aggregation area was mainly distributed in the northwestern and central areas, the low-value aggregation area distribution was more dispersed, with broken distribution, and accompanied by a small part of the low–high aggregation area; the C/N high-value aggregation area was distributed in the northwest, and the low-value aggregation area distribution was dispersed and accompanied by a small part of the low–high aggregation area. The C/N high-value aggregation area was distributed in the northwestern part and the low-value aggregation area was distributed in the southern part of the study area, which was fragmented and accompanied by a small portion of the high–low aggregation area.

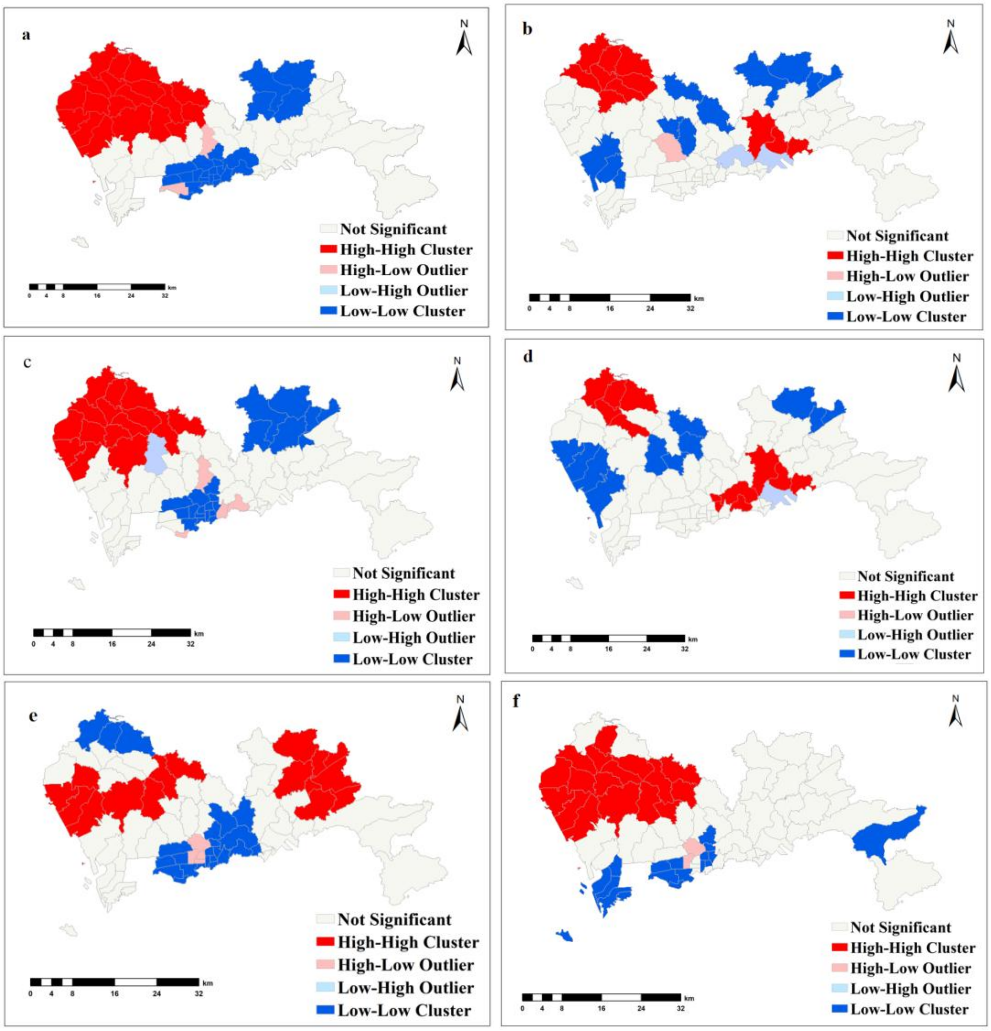

Figure 2. LISA clustering maps of SOC, TN, and C/N in forest soils of Shenzhen City, China. Note: (**a**,**c**,**e**) represent the distribution of SOC, TN and C/N spatial outliers at 0–10 cm of soil, respectively. (**b**,**d**,**f**) represent the distribution of SOC, TN and C/N outliers at 10–30 cm of soil, respectively.

3.4. Patterns of Spatial Distribution of SOC, TN, and C/N

According to the parameters of the semi-ANOVA results, the spatial distribution map was drawn using the ordinary Kriging interpolation method of ArcGIS 10.8 (Figure 3). The high-value area of 0–10 cm SOC content was mainly distributed in the northwest with a patchy distribution phenomenon, whereas the low-value area was mainly distributed in the north and the south-central area with a block distribution; the TN content was similar to the distribution of SOC; the high-value area of C/N was mainly distributed in the west with a strip distribution, and the low-value area was distributed in the edges of the study area with fragmentation; the high-value area of 10–30 cm SOC content was mainly distributed in the southeast with a strip distribution. Low-value zones were mainly distributed in the north, high-value zones of TN content were mainly distributed in the eastern part of the south, low-value zones were mainly distributed in the north and west, high-value zones of C/N content were mainly distributed in the western and northwestern parts of the study area, and low-value zones were mainly distributed in the eastern part of the study area.

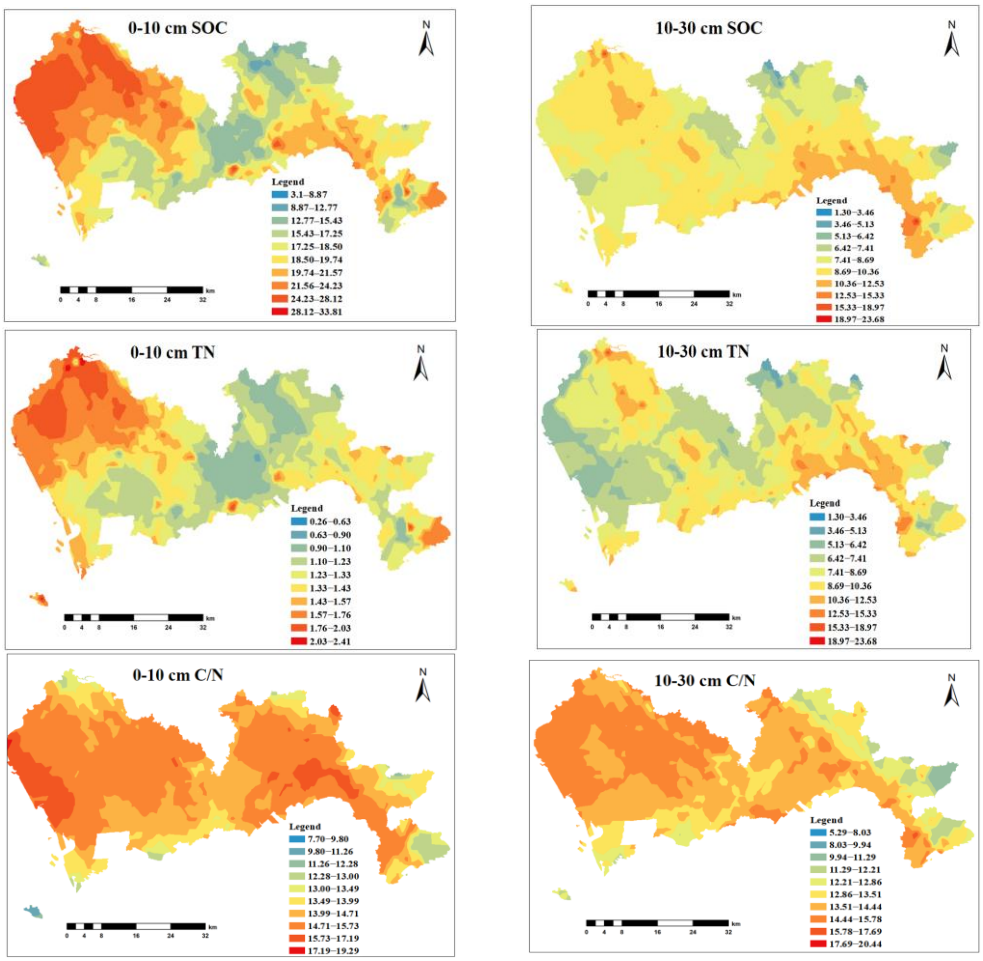

Figure 3. Spatial distribution of SOC, TN, and C/N in forest soils of the study area in Shenzhen City, China.

3.5. Correlation Analysis of SOC, TN, and C/N with Impact Factors

The results of correlation analysis of climatic, vegetative, anthropogenic and soil factors with SOC, TN, and C/N in the study area (Figure 4) showed that the 0–10 cm SOC showed highly significant positive correlations ($p < 0.01$) with depression, conductivity, and TN; significant positive correlations ($p < 0.05$) with C/N; and highly significant negative correlations ($p < 0.01$) with soil bulk weight, soil TN and depression, conductivity and SOC ($p < 0.01$), elevation ($p < 0.05$), soil bulk density ($p < 0.01$), and annual rainfall and

average annual air temperature ($p < 0.01$). C/N was positively correlated with nighttime light index ($p < 0.05$), and average annual rainfall and air temperature ($p < 0.01$). SOC from the 10–30 cm layer was significantly positively correlated with elevation, TN, and C/N ($p < 0.01$); significantly positively correlated with depression, conductivity, agglomeration (1–0.5 mm), and vegetation primary productivity ($p < 0.05$); and negatively correlated with soil bulk weight ($p < 0.01$) and GWD ($p < 0.05$). TN was negatively correlated with nighttime light index ($p < 0.05$), and mean annual rainfall and air temperature ($p < 0.05$); TN was significantly positively correlated with nighttime light index ($p < 0.05$), and mean annual rainfall and air temperature ($p < 0.05$); TN was significantly and positively correlated with slope, depression, and conductivity ($p < 0.05$) and significantly and negatively correlated with soil bulk weight ($p < 0.01$); and C/N was significantly and negatively correlated with pH ($p < 0.05$).

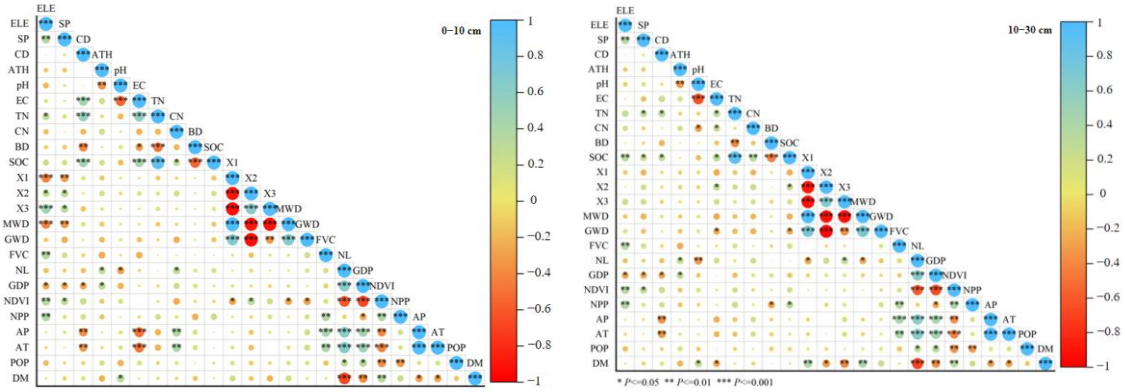

Figure 4. Correlation coefficients between SOC, TN, C/N and influencing factors in forest soils of Shenzhen City, China.

To further reveal the relative contributions of the influencing factors to SOC, TN, and C/N, redundancy analysis was used to investigate the relative contribution of each factor (Figure 5). The 0–10 cm results showed that the variance contribution of the first axis reached 54.54% and the cumulative variance contribution reached 58.86%. Among them, the arrows for soil bulk density (BD), electrical conductivity (EC), depression (CD), and average annual rainfall (AP) had longer connecting lengths, indicating that these factors played a better role in explaining the 0–10 cm SOC, TN, and C/N. Moreover, the cosine values showed that SOC, TN, and C/N were significantly and negatively correlated with soil bulk weight and significantly and positively correlated with conductivity and depression, and that C/N was significantly and positively correlated with average annual rainfall (AP). The 10–30 cm results showed that the contribution of the variance of the first axis reached 41.39%, and the cumulative contribution of the variance reached 46.95%. Three of these, pH, soil BD, and slope (SP), had a strong influence; SOC, TN, and C/N were negatively correlated with pH and soil BD, and SOC and TN were positively correlated with SP. The factor scores of the component matrix indicated that the soil capacity weight was the highest and was the main influencing factor.

3.6. Differences in SOC, TN, and C/N Across Vegetation Types

Analysis of variance (ANOVA) and post-event comparative testing (Duncan) for SOC, TN, and C/N in different vegetation types (Table 4) showed that there were no significant differences among SOC, TN, and C/N at soil depths of 0–10 cm ($p > 0.05$); in soil depths of 0–10 cm, the SOC contents were in the order of coniferous forests > secondary broadleaf forests > broadleaf plantation forests, the coniferous forests were significantly higher than the second-growth broadleaf forests ($p < 0.05$), and the TN and C/N values were not significantly different among the different vegetation types ($p > 0.05$).

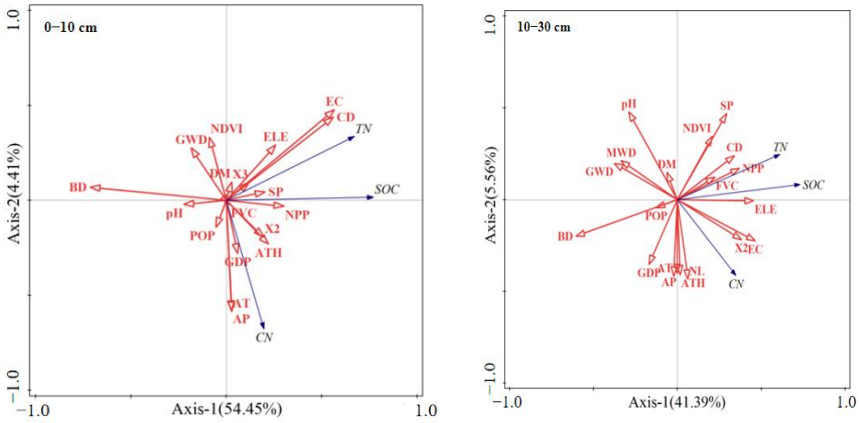

Figure 5. Redundancy Analysis of SOC, TN, C/N and influencing factors in forest soils of Shenzhen City, China.

Table 4. SOC, TN, and C/N contents in 0–10 cm and 10–30 cm forest soils under different vegetation types in Shenzhen City, China.

Vegetation Type	Soil Depth/(cm)	SOC/(g·kg^{-1})	TN (g·kg^{-1})	C/N
Secondary broadleaf forest	0–10	18.40 ± 7.39 a	1.28 ± 0.48 a	14.39 ± 2.00 a
	10–30	9.56 ± 3.82 ab	0.71 ± 0.26 a	13.38 ± 2.69 a
Broad-leaved plantation	0–10	18.62 ± 6.29 a	1.29 ± 0.46 a	14.69 ± 2.11 a
	10–30	8.00 ± 3.11 b	0.58 ± 0.23 a	13.94 ± 2.18 a
Coniferous forests	0–10	17.25 ± 8.01 a	1.31 ± 0.63 a	13.86 ± 3.46 a
	10–30	11.28 ± 6.69 a	0.78 ± 0.39 a	14.55 ± 3.78 a

Note: The data in the table are mean ± standard deviations, and different lowercase letters in the same column after the data indicate significant differences ($p < 0.05$).

3.7. Regression Analysis of SOC, TN, and C/N with Environmental Factors

Regression analysis was used to quantitatively express and test the degree of influence of climatic, geomorphic, anthropogenic, vegetation, and soil factors on SOC, TN, and C/N of forest soils in Shenzhen. The stepwise regression method was used to analyze the effects of influencing factors on SOC, TN, and C/N, and was combined with the VIF value to test the problem of covariance of independent variables. Table 5 shows that the VIF values are all <10; therefore, the problem of covariance of independent variables is excluded; the R2 of regression variance of SOC, TN, and C/N for the 0–10 cm and 10–30 cm soil layers were 0.43, 0.48, and 0.87, and 0.39, 0.24, and 0.81, respectively. Overall, these factors had a greater effect on SOC and TN, but the degree of explanation was not high, and that for C/N was higher.

Combining the regression analysis and the decomposition of the relative importance of key factors, it can be seen (Figure 6) that in 0–10 cm soil, the ranking of contributing factors to SOC variation were BD (52.8%), EC (38.6%), and AP (8.6%), and the climate factor only contributed 8.6%, indicating that the soil factor was the key factor influencing the SOC content of soil, with BD being the key factor. The order of contributing factors to TN variation was EC (36.01%), CD (27.53%), BD (23.88%), and ELE (12.59%), geomorphological factors contributed 12.59%, and the soil factor explained 87.41% of the variation, of which EC was the key factor influencing soil TN. The order of contributing factors to C/N variation was TN (47.58%) SOC (44.33%), GWD (4.01%), BD (3.52%), and SP (0.55%), and the variation in C/N was mainly from the soil factors, whereas C/N was closely related to SOC and TN, GWD and SP had a significant effect on C/N ($p < 0.01$), and the effect of slope on the surface C/N of the soil was also considered in the subsequent study. In the 10–30 cm soil, the contributing factors to SOC variation were ranked as BD (51.42%), ELE (28.47%),

and GWD (20.11%). BD was also a key factor influencing SOC in the deeper soil layers, and the deeper SOC content increased significantly with increasing elevation and decreased significantly with increasing GWD ($p < 0.01$). Factors contributing to TN variation in the 10–30 cm soil were ranked as BD (51.42%), ELE (28.47%), and GWD (20.11%). The effects of slope were also considered in subsequent studies. Contributing factors in the 10–30 cm soil were ranked as BD (52.18%), EC (25.31%), and ELE (22.51%), in which elevation had a significant positive effect on TN ($p < 0.01$). Contributing factors to C/N variation in the 10–30 cm soil were ranked as SOC (52.03%), TN (40.98%), EC (5.74%), and NDVI (1.25%), consistent with the key drivers of C/N in surface soil. SOC and TN were the key drivers of C/N in the 10–30 cm soil, and the NDVI became one of the factors that significantly influenced C/N.

3.8. Structural Equation Analysis of SOC, TN, and C/N Using the Partial Least Squares Method

Partial Least Squares Structural Equation Modeling was used to quantify the direct and indirect effects of climate, human activities, geomorphology, vegetation, and soil factors on SOC, TN, and C/N of forest soils in Shenzhen through the pathway system. The driving mechanisms of SOC, TN, and C/N were analyzed in the context of the geographic differentiation of Shenzhen, which is characterized by "Northwest hilly woodland-central urban core-southern coastal urban area" (Figure 7).

Table 5. Results of regression analysis between SOC, TN, C/N and different influencing factors in 0–10 cm and 10–30 cm forest soils of Shenzhen City, China.

	Depth Soil/cm	Impact Factor	Non-Standardized Coefficient		Standardized Coefficient	t	*p*	VIF	R^2	Adj. R^2	AIC	BIC	F
			B	Standard Error	Beta								
SOC	0–10	/	31.16	9.27	0.00	3.36	0.001 ***	-	0.46	0.43	397.6	408.31	F = 16.346, *p* = 0.000 ***
		BD	−25.70	5.86	−0.45	−4.39	0.000 ***	1.10					
		EC	119.19	29.59	0.48	4.03	0.000 ***	1.48					
		AP	0.00	0.00	0.32	2.81	0.007 ***	1.37					
TN		/	1.42	0.61	0.00	2.32	0.024 **	-	0.52	0.48	53.65	66.51	F = 14.982, *p* = 0.000 ***
		EC	5.99	1.85	0.35	3.24	0.002 ***	1.32					
		BD	−1.00	0.41	−0.25	−2.43	0.018 **	1.23					
		ELE	0.00	0.00	0.23	2.49	0.016 **	1.02					
		CD	0.69	0.29	0.26	2.35	0.023 **	1.42					
C/N		/	26.75	5.10	0.00	5.25	0.000 ***	-	0.88	0.87	160.72	173.58	F = 83.078, *p* = 0.000 ***
		GWD	−3.31	1.57	−0.10	−2.11	0.040 **	1.09					
		BD	−1.37	1.03	−0.07	−1.33	0.190	1.44					
		TN	−8.67	0.46	−1.86	−19.01	0.000 ***	4.49					
		SOC	0.60	0.03	1.86	17.91	0.000 ***	5.06					
		SP	−0.02	0.01	−0.12	−2.44	0.018 **	1.08					
SOC	10–30	/	80.36	16.48	0.00	4.88	0.000 ***	-	0.42	0.39	334.44	345.16	F = 13.629, *p* = 0.000 ***
		BD	−18.21	3.93	−0.47	−4.63	0.000 ***	1.00					
		ELE	0.01	0.00	0.36	3.54	0.001 ***	1.01					
		GWD	−16.24	5.16	−0.32	−3.15	0.003 ***	1.02					
TN		/	1.58	0.43	0.00	3.70	0.000 ***	-	0.28	0.24	6.55	17.26	F = 7.414, *p* = 0.000 ***
		BD	−0.93	0.29	−0.37	−3.22	0.002 ***	1.02					
		ELE	0.00	0.00	0.25	2.23	0.030 **	1.00					
		EC	4.43	2.06	0.24	2.15	0.036 **	1.02					
C/N		/	14.46	1.02	0.00	14.18	0.000 ***	-	0.82	0.81	208.93	221.79	F = 65.42, *p* = 0.000 ***
		SOC	1.29	0.08	1.99	15.30	0.000 ***	5.39					
		TN	−18.51	1.27	−1.87	−14.56	0.000 ***	5.25					
		EC	29.32	10.65	0.16	2.75	0.008 ***	1.12					
		NDVI	−2.40	1.10	−0.12	−2.17	0.034 **	1.03					

Note: *p*-values are ** $p < 0.01$; *** $p < 0.001$.

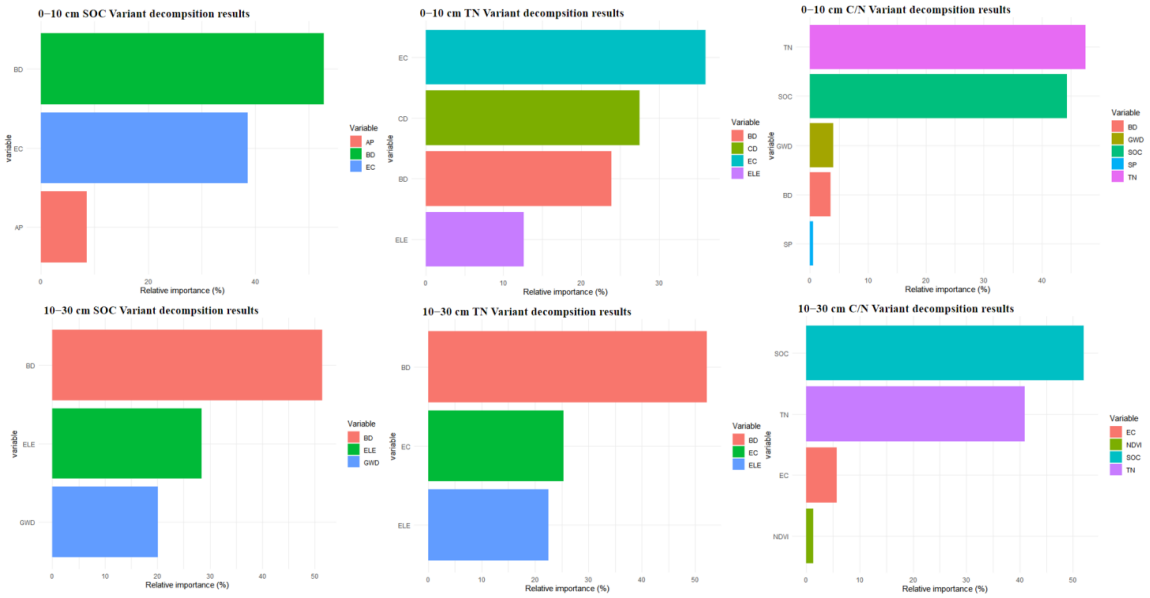

Figure 6. Relative importance of different influencing factors on SOC, TN, and C/N in forest soils of Shenzhen City, China.

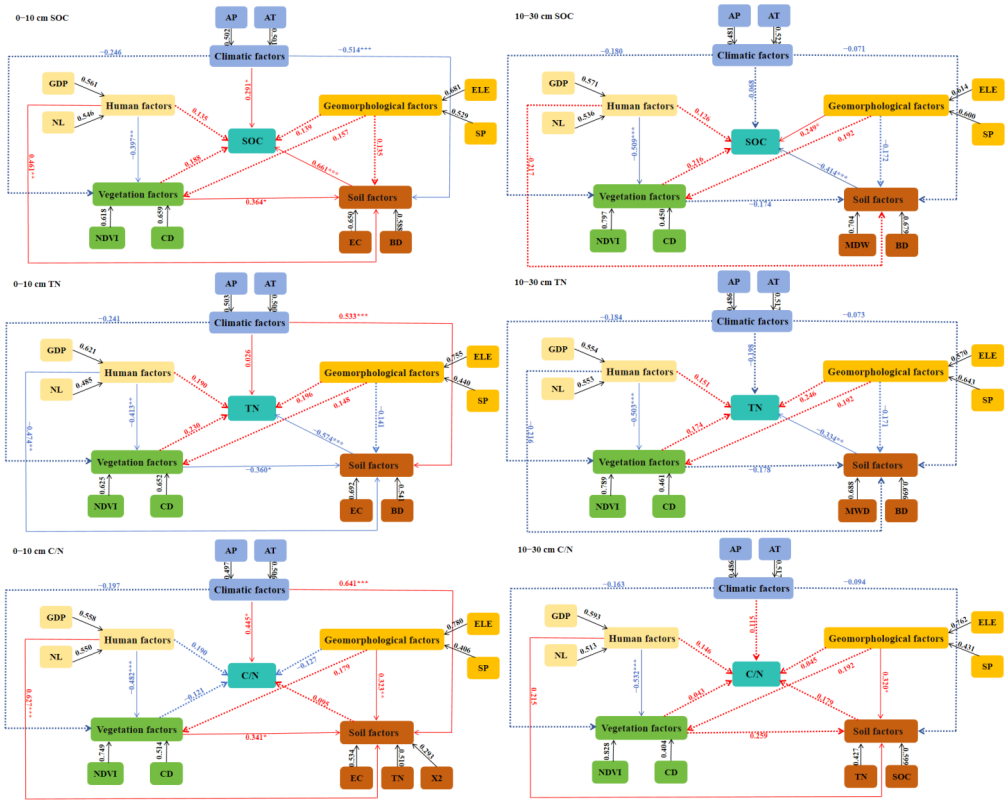

Figure 7. Partial Least Squares Structural Equation Modeling of environmental variables and SOC, TN, C/N in forest soils of Shenzhen City, China. Note: Each box in the figure represents a latent variable. AP denotes average annual rainfall, AT denotes average annual temperature, ELE denotes elevation, SP denotes slope, GDP denotes Gross Domestic Product, NL denotes nighttime light index, NDVI denotes Normalized Vegetation Index, CD denotes Depression, EC denotes Electrical Conductivity, BD denotes Soil Bulk Weight, MWD denotes Mean Weight Diameter, and X2 denotes Aggregates 1–0.5 mm. Numbers on arrows are for effect sizes; a solid line indicates a significant effect, a dashed line indicates no significant effect; red indicates a positive effect, blue indicates a negative effect. *p*-values are: * $p < 0.05$; ** $p < 0.01$; *** $p < 0.001$.

4. Discussion

4.1. Characterization of SOC, TN, and C/N and Spatial Distribution

In this study, the spatial distribution characteristics of SOC, TN, and C/N at depths of 0–10 cm and 10–30 cm were systematically analyzed based on forest soil survey data in Shenzhen. The mean values of SOC, TN, and C/N were 18.32 $g \cdot kg^{-1}$, 1.29 $g \cdot kg^{-1}$, and 14.43 at a 0–10 cm depth, and 9.24 $g \cdot kg^{-1}$, 0.67 $g \cdot kg^{-1}$, and 13.75 at a 10–30 cm depth, respectively. Compared with the grading standards of properties of the second national soil census, the SOC and TN of the 0–10 cm soils were Grades 2 (medium-high) and 3 (medium), respectively, whereas at a depth of 10–30 cm, the SOC and TN dropped to Grades 4 (medium-low) and 5 (low), respectively. Compared with the national averages (9.27 $g \cdot kg^{-1}$ for SOC, 0.76 $g \cdot kg^{-1}$ for TN, and 11.9 for C/N), the surface SOC and TN were significantly higher than the national values; however, the sub-surface layer (10–30 cm) was lower than the national levels for SOC and TN, and higher than the national values for C/N. This vertical differentiation suggests that carbon and nitrogen accumulation in the surface layer was dominated by recent biological processes, whereas the subsurface layer was more significantly influenced by historical legacies and leaching [28,29]. In Shenzhen's urban forests, there were no significant differences in SOC, TN, and C/N contents among different vegetation types in the 0–10 cm soil layer ($p > 0.05$); only in the 10–30 cm soil layer was the SOC content of coniferous forests significantly higher than that of artificial broad-leaved forests. This phenomenon may be attributed to the intense anthropogenic disturbances in Shenzhen's urban forests, which have weakened the differences in vegetation type-induced carbon and nitrogen inputs to the surface soil. In contrast, the subsurface soil is less affected by human activities: the higher lignin content in the litter of coniferous forests retards decomposition, making it easier to form SOC accumulation [15]. In the context of urbanization, the impact of anthropogenic management on carbon and nitrogen in the topsoil often outweighs that of vegetation itself, while the subsurface soil is better able to retain the differential signals generated by the decomposition of vegetation litter [28].

4.2. Analysis of Spatial Distribution Characteristics and Anomaly Formation Mechanism

The SOC, TN, and C/N ratio of forest soils in Shenzhen were unevenly distributed throughout the region, showing strong spatial variability. The semi-variance function analysis revealed that the block-base ratios of SOC and TN were both <25%, indicating strong spatial autocorrelation, and their variability was mainly controlled by structural factors. In contrast, the block-base ratios of C/N were >75%, indicating weak spatial autocorrelation, and the variability was mainly driven by stochastic factors. This pattern is consistent with the global pattern of soil variability, in which structural factors dominate carbon and nitrogen parameters, whereas C/N is susceptible to short-term perturbations [30]. The ranges of SOC, TN, and C/N at a 0–10 cm depth were 2443 m, 864 m, and 11,032 m, respectively, whereas those at a 10–30 cm depth were 6949 m, 21,330 m, and 12,381 m, respectively. The range of C/N was the largest (>11,000 m), which indicated that its spatial continuity was large and might have been due to the influence of wide-area vegetation or hydrological processes, whereas TN was smaller (<900 m), indicating that it was more susceptible to localized nitrogen input or loss, reflecting greater susceptibility to disturbance by localized N inputs or losses. This difference in the range highlights the spatial-scale dependence of the C/N ratio as an indicator of ecosystem stability [31]. Moran's *I* index analysis showed highly significant spatial autocorrelation ($p < 0.001$) for SOC, TN, and C/N at different depths, indicating an aggregated rather than random pattern of distribution across the region. This is consistent with the patchy pattern of topography and land use in Shenzhen, and verifies the generalizability of spatial autocorrelation in soil parameters [32,33].

The LISA map shows that the SOC high–low anomaly area is concentrated in the central urban built-up area. In this region, the SOC is generally low because of soil compaction and vegetation destruction caused by high-density construction in the urban core area [34]; however, large parks have developed localized high SOC values through long-term artificial maintenance, which constitute a stark contrast to the surrounding low value areas [35]. This "insular green space" effect highlights the role of anthropogenic management in regulating urban soil carbon pools [36]. The 0–10 cm TN high–low anomaly area was distributed in the southern urbanized high-intensity zone. Industrial pollution and impervious surface obstruction in this area generally result in low TN [37,38]; however, the input of nitrogen from point sources, such as artificial wetlands, increases the local TN and forms an anomaly. The 10–30 cm C/N ratio showed high and low anomalies in the reclaimed land in the southern part of the country, where the high pH caused by reclamation accelerated the decomposition of organic matter, and the C/N ratio was generally low. However, the local soil characteristics could raise the C/N ratio, which reflects the disturbance of nitrogen cycling caused by stochastic factors. The 0–10 cm SOC and TN high-value zones were mainly in a patchy pattern, whereas the high-value zone in the northwestern part of the low mountainous hilly region was mainly in a patchy pattern. The high value areas of 0–10 cm SOC and TN are mainly distributed in patches in the northwestern low mountainous and hilly areas. The high vegetation cover in this area is rich in apoplastic inputs, and the water-saturated state of the marshy saline soil inhibits microbial decomposition and promotes the accumulation of SOC. In contrast, urbanization in the south-central plains led to the destruction of vegetation and the reduction in SOC inputs, while agricultural activities in the northern hills accelerated the mineralization of organic matter. TN and SOC were highly coupled, suggesting that organic matter inputs synchronously drove the accumulation of carbon and nitrogen, and that organic matter was simultaneously lost in the face of disturbances, which was consistent with studies in other regions. The patterns of soil carbon and nitrogen at depths of 0–30 cm were the result of the superposition of long-term natural processes and human activities. Natural woodlands in the southeast, dominated by low-disturbance hills and mature forests, have high root biomass and rich lignin content, which promote the continuous accumulation of SOC and TN in the deep layer through apoptotic decomposition and vertical migration, reflecting the carbon sink function of natural vegetation [39]. Northern industrial areas, such as electronics manufacturing and other industries, lead to the destruction of the soil structure, and SOC and TN are lost through topsoil stripping, highlighting the negative impacts of high-intensity anthropogenic disturbances. West mangrove belt: High C/N of apomictic material and an anaerobic environment formed by tidal deposition, which inhibits the nitrogen decomposition rate and leads to C/N elevation. Simultaneously, river scouring accelerates nitrogen leaching, further increasing C/N [40]. Artificial green spaces and agricultural fields at the edges of the study area increased nitrogen inputs and decreased C/N owing to apomictic clearing and fertilization, reflecting the bidirectional effects of human management.

4.3. Analysis of Factors Affecting SOC, TN, and C/N

Exploring the spatial distribution and driving mechanisms of SOC, TN, and C/N in urban forest soils is conducive to the accurate, scientific, and sustainable management of urban soils and the enhancement of their ecological service functions. The results of this study showed that climate, topography, vegetation, anthropogenic, and soil factors all influence the spatial distribution of SOC, TN, and C/N in forest soils.

SOC from the 0–10 cm was significantly correlated with depression, conductivity, and soil bulk weight, which were influenced by climatic and soil factors. Soil bulk weight was

the main controlling factor affecting SOC content. The increase in soil bulk density leads to a decrease in soil porosity, deterioration of soil structure, decrease in water infiltration, impediment of plant fine root growth and nutrient cycling, and weakening of the organic matter regeneration ability [41]. Simultaneously, the large amount of apoplastic litter accumulated on the soil surface provided more soluble organic carbon, which stimulated soil microbial activities and promoted the decomposition of carbon in the soil. TN was significantly correlated with elevation, depression, electrical conductivity, soil bulk weight, average annual rainfall, and average annual air temperature, and was affected by climatic, vegetation, and soil factors. Soil electrical conductivity was the main controlling factor affecting soil TN content. C/N was significantly correlated with SOC, nighttime light index, mean annual rainfall, and mean annual air temperature. C/N was influenced by topographic and soil factors, and SOC and TN were the main controlling factors affecting soil C/N content. In addition, C/N was significantly and positively correlated with the nighttime light index ($p < 0.05$), which can characterize the intensity of human activities and is suitable for monitoring human behavioral activities and urban development dynamics [42]. 10–30 cm SOC and TN were affected by topographic and soil factors, and soil bulk density was the dominant factor affecting TN; C/N was affected by soil and vegetation factors, and SOC and TN were the dominant factors affecting C/N.

Partial least squares structural equation modeling showed that soil factors were the main drivers of changes in SOC content at soil depths of 0–10 cm, with conductivity and soil bulk weight being the core variables. The combination of these two factors made soil factors the primary driver of surface SOC. Second, climatic factors had a direct and positive effect on SOC, with mean annual rainfall and mean annual air temperature being the core variables. Climatic factors can also affect SOC by influencing soil factors. Rainfall increases soil water content to promote lubrication between soil particles and reduce friction between soil particles, thus reducing soil bulk density and removing fine particles and soluble salts from the soil through leaching, which not only reduces bulk density but also reduces electrical conductivity. As the soil factor is the main driving factor of TN content change, Shenzhen is a highly urbanized city, nitrogen deposition is significant, and high temperatures and rainfall are accompanied by nitrogen influx into the soil; thus, the TN content of the soil increased significantly. Climatic factors have a direct and positive effect on soil C/N. In addition, the effects of human activities on SOC, TN, and C/N ratios cannot be ignored. Although the direct effect of anthropogenic activities was not significant, as shown in the pathway, anthropogenic activities can indirectly affect changes in SOC and TN content by affecting vegetation and soil. In the modeling of SOC and C/N, it was found that human activities positively affected both soil factors Human activities mainly affected soil capacity in the form of trampling, and severe trampling led to a significant increase in soil capacity [43]. Anthropogenic activity had a significant negative effect ($p < 0.01$) on all the vegetation factors. Soil compactness leads to difficulties in gas exchange and reduced microbial activity, resulting in a lower rate of organic matter mineralization and a build-up of elemental carbon, which leads to higher C/N values [44]. The key drivers of SOC and TN at 10–30 cm were still soil factors, and topographic factors also had a direct positive effect ($p < 0.05$) on changes in SOC content. Surface SOC was mainly derived from apoplastic decomposition, which was susceptible to climatic and vegetative disturbances, weakening the influence of topography, whereas urban forest surface soils were more susceptible to anthropogenic disturbances, all of which may mask the effects of elevation and slope.

5. Conclusions

In this study, the spatial distribution characteristics of SOC, TN, and C/N and their influencing factors were revealed using multivariate statistics and spatial analysis in the

0–10 cm and 10–30 cm soil layers of forest soils in Shenzhen. The SOC and TN contents of forest soils in Shenzhen showed obvious epistatic characteristics, and the average SOC and TN values in the 0–10 cm soil layer were significantly higher than those in the 10–30 cm soil layer. The differences in C/N in the two soil layers were small. In the spatial distribution, the high-value areas of 0–10 cm SOC and TN were concentrated in the northwestern low hills, and the low-value areas were mainly distributed in the northern and south-central areas, which were distributed in a block shape. The high value areas of 10–30 cm SOC were extended to the southeast, and the low-value areas were mainly distributed in the northern part of the country. The high-value areas of TN were extended to the southeast, and the low value areas were distributed in the northern and western parts of the country. The high value areas of C/N were mainly distributed in the western and northwestern parts of the country. The low-value zones in the 0–10 cm and 10–30 cm soil layers were distributed at the edges and southern part of the study area, respectively, in a fragmented manner.

SOC, TN, and C/N showed moderate spatial variability. Among them, SOC and TN had high spatial autocorrelation, and their spatial variability was mainly controlled by structural factors, such as parent material and topography, whereas C/N had weak spatial autocorrelation, and its variability was more influenced by random factors. Spatial variations in SOC, TN, and C/N were the result of the joint action of natural and anthropogenic factors; however, the main controlling factors varied in different soil layers. In the 0–10 cm soil layer, soil bulk density and conductivity were the key factors affecting SOC and TN, whereas C/N was mainly regulated by the coupling relationship between SOC and TN. In the 10–30 cm soil layer, elevation and soil bulk density had a more significant effect on SOC and TN, and C/N was mainly regulated by the coupling relationship between SOC and TN. In the 10–30 cm soil layer, elevation and soil bulk weight had more significant effects on SOC and TN, whereas C/N was closely related to SOC, TN, and the normalized vegetation index. Anthropogenic factors mainly affect the C/N ratio by interfering with the carbon and nitrogen balances of the surface soil.

This study clarified the spatial patterns and driving mechanisms of soil carbon and nitrogen in the forests of Shenzhen City, providing a scientific basis for the improvement of soil fertility, optimization of carbon sink functions, and ecosystem management in urban forests. Meanwhile, some variability was noted in the importance ranking of the influencing factors of SOC and TN in the surface and subsurface soils, which requires targeted measures for protection and restoration. In a follow-up study, the sample size should be further expanded and combined with long-term positional monitoring and in-depth exploration of the dynamic impact of urbanization on soil carbon and nitrogen cycles.

Author Contributions: Conceptualization, Z.D.; methodology, Z.D. and S.D.; software, W.Z. and X.M.; validation, Z.D.; formal analysis, Z.D.; investigation, H.X.; resources, Z.S.; data curation, Z.D. and Z.S.; writing—original draft preparation, Z.D.; writing—review and editing, H.X.; visualization, Z.D.; supervision, Z.D.; project administration, Z.S.; funding acquisition, Z.S. All authors have read and agreed to the published version of the manuscript.

Funding: This work was funded by the Shenzhen Science and Technology Program (KCXST20221021111211025).

Data Availability Statement: The raw data supporting the conclusions of this article will be made available by the authors on request.

Acknowledgments: All of the authors especially appreciate Qinghai Normal University and Fairylake Botanical Garden. We thank the editors and anonymous reviewers for their valuable comments.

Conflicts of Interest: The authors declare no conflicts of interest.

References

1. Don, A.; Schumacher, J.; Freibauer, A. Impact of tropical land-use change on soil organic carbon stocks—A meta-analysis. *Glob. Change Biol.* **2011**, *17*, 1658–1670. [CrossRef]
2. Bae, J.; Ryu, Y. Land use and land cover changes explain spatial and temporal variations of the soil organic carbon stocks in a constructed urban park. *Landsc. Urban Plan.* **2015**, *136*, 57–67. [CrossRef]
3. Chen, F.-S.; Yavitt, J.; Hu, X.-F. Phosphorus enrichment helps increase soil carbon mineralization in vegetation along an urban-to-rural gradient, Nanchang, China. *Appl. Soil Ecol.* **2014**, *75*, 181–188. [CrossRef]
4. Li, T.; Zheng, W.; Zhang, S.; Jia, Y.; Li, Y.; Xu, X. Spatial variations in soil phosphorus along a gradient of central city-suburb-exurban satellite. *Catena* **2018**, *170*, 150–158. [CrossRef]
5. O'Brien, L.E.; Urbanek, R.E.; Gregory, J.D. Ecological functions and human benefits of urban forests. *Urban For. Urban Green.* **2022**, *75*, 127707. [CrossRef]
6. Fang, X.; An, S.S.; Xue, Z.L.; Li, B.C. Small watersheds of the Loess Plateau based on maximum likelihood and moment methods Spatial variation analysis of soil carbon and nitrogen. *Bull. Soil Water Conserv.* **2014**, *34*, 141–146. [CrossRef]
7. Setälä, H.M.; Francini, G.; Allen, J.A.; Hui, N.; Jumpponen, A.; Kotze, D.J. Vegetation type and age drive changes in soil properties, nitrogen and carbon sequestration in urban parks under cold climate. *Front. Ecol. Evol.* **2016**, *4*, 93. [CrossRef]
8. Gregorich, E.G.; McLaughlin, N.B.; Lapen, D.R.; Ma, B.L.; Rochette, P. Soil Compaction, Both an Environmental and Agronomic Culprit: Increased Nitrous Oxide Emissions and Reduced Plant Nitrogen Uptake. *Soil Sci. Soc. Am. J.* **2014**, *78*, 1913–1923. [CrossRef]
9. Guo, B.X.; Zhou, J.; Zhan, L.Q.; Wang, Z.Y.; Wu, W.; Liu, H.B. Spatial and Temporal Variability of Soil pH, Organic Matter and Available Nutrients (N, P and K) in Southwestern China. *Agronomy* **2024**, *14*, 1796. [CrossRef]
10. Hadole, S.S.; Sarap, P.A.; Sarode, M.D.; Reddy, Y.A.; Padekar, P.D.; Dhule, D.T.; Dangore, S.T. Assessment of Spatial Variability of Major and Micro Nutrients in Soils of Satara District, Maharashtra, India. *Int. J. Plant Soil Sci.* **2024**, *36*, 541–552. [CrossRef]
11. Lal, R. Soil Carbon Sequestration Impacts on Global Climate Change and Food Security. *Science* **2004**, *304*, 1623–1627. [CrossRef]
12. Lili, Y.; Ning, M. Empirical Study on the Influence of Urban Environmental Industrial Structure Optimization on Ecological Landscape Greening Construction. *Int. J. Environ. Res. Public Health* **2022**, *19*, 16842. [CrossRef]
13. Liu, D.; Wang, Z.; Zhang, B.; Song, K.; Li, X.; Li, J.; Li, F.; Duan, H. Spatial distribution of soil organic carbon and analysis of related factors in croplands of the black soil region, Northeast China. *Agric. Ecosyst. Environ.* **2005**, *113*, 73–81. [CrossRef]
14. Liu, Q.Q.; Li, W.S.; Liu, X.; Dong, L.N.; Zhao, C.; Leng, H.M.; Liu, X.; Zhang, J.C. Effects of stampede on the species composition and diversity of vegetation in the herbaceous layer of urban forests and the physical and chemical properties of soil. *J. Northeast. For. Univ.* **2024**, *52*, 117–124. [CrossRef]
15. Liu, W.L.; Zhang, L.B.; Ye, Y.H.; Zou, J.F.; Wang, Y.Z.; Qi, Y. The content and density of soil organic carbon under different land use types in Shenzhen. *Ecol. Sci.* **2011**, *30*, 486–492.
16. Lu, Y.; Zhuang, J.; Yang, C.; Li, L.; Kong, M. How the digital economy promotes urban–rural integration through optimizing factor allocation: Theoretical mechanisms and evidence from China. *Front. Sustain. Food Syst.* **2025**, *9*, 1494247. [CrossRef]
17. Santos-Andrade, M.; Hatje, V.; AriasOrtiz, A.; Patire, V.F.; da Silva, L.A. Human disturbance drives loss of soil organic matter and changes its stability and sources in mangroves. *Environ. Res.* **2021**, *202*, 111663. [CrossRef] [PubMed]
18. Zhang, S.; Zhou, X.; Chen, Y.; Du, F.; Zhu, B. Soil organic carbon fractions in China: Spatial distribution, drivers, and future changes. *Sci. Total Environ.* **2024**, *919*, 170890. [CrossRef]
19. Jiwen, C.; Ruili, Z.; Xiya, W.; Xinpeng, X.; Chao, A.; Ping, H.; Guoqing, L.; Wei, Z.; Ping, Z. Effect of high soil C/N ratio and nitrogen limitation caused by the long-term combined organic-inorganic fertilization on the soil microbial community structure and its dominated SOC decomposition. *J. Environ. Manag.* **2022**, *303*, 114155. [CrossRef]
20. Niemelä, J.; Saarela, S.-R.; Söderman, T.; Kopperoinen, L.; Yli-Pelkonen, V.; Väre, S.; Kotze, D.J. Using the ecosystem services approach for better planning and conservation of urban green spaces: A Finland case study. *Biodivers. Conserv.* **2010**, *19*, 3225–3243. [CrossRef]
21. Nowak, D.J.; Greenfield, E.J.; Hoehn, R.E.; Lapoint, E. Carbon storage and sequestration by trees in urban and community areas of the United States. *Environ. Pollut.* **2013**, *178*, 229–236. [CrossRef]
22. Nyamadzawo, G.; Shukla, M.K.; Lal, R. Spatial variability of total soil carbon and nitrogen stocks for some reclaimed minesoils of southeastern Ohio. *Land Degrad. Dev.* **2008**, *19*, 275–288. [CrossRef]
23. Qian, F.; Yu, Y.; Dong, X.; Gu, H. Soil Quality Evaluation Based on a Minimum Data Set (MDS)—A Case Study of Tieling County, Northeast China. *Land* **2023**, *12*, 1263. [CrossRef]
24. Jing, Z.; Miao, Z.; Shaoyan, H.; Xuan, Z. Assessing spatial variability of soil organic carbon and total nitrogen in eroded hilly region of subtropical China. *PLoS ONE* **2020**, *15*, e0244322. [CrossRef]
25. Ginestet, C. ggplot2: Elegant Graphics for Data Analysis. *J. Stat. Softw.* **2011**, *174*, 245–246. [CrossRef]
26. Gromping, U. Relative Importance for Linear Regression in R: The Package relaimpo. *J. Stat. Softw.* **2006**, *17*, 1–27. [CrossRef]

27. Min-Suk, K.; Sang-Hwan, L.; Jeong-Gyu, K. Evaluation of factors affecting arsenic uptake by Brassica juncea in alkali soil after biochar application using partial least squares path modeling (PLS-PM). *Chemosphere* **2021**, *275*, 130095. [CrossRef]
28. Ramon, M.; Lafortezza, R.; Ribeiro, A.P.; Camargo, P.B.d.; Domingos, M.; Gomes, E.P.C.; Tavares, A.d.R.; Dias, A.G.; Kniess, C.T.; Ferreira, M.L. Carbon and nitrogen stock in soils of subtropical urban forests: Isotopic δ13C and δ15N indicators for nature-based solutions in a megacity. *Ecol. Indic.* **2024**, *160*, 111743. [CrossRef]
29. Kiran, G.S.; Kinnary, S. Carbon Sequestration by Urban Trees on Roadsides of Vadodara City. *Int. J. Eng. Sci. Technol.* **2011**, *3*, 3066.
30. Semenov, M.Y.; Silaev, A.V.; Semenov, Y.M.; Begunova, L.A.; Semenov, Y.M. Identifying and Characterizing Critical Source Areas of Organic and Inorganic Pollutants in Urban Agglomeration in Lake Baikal Watershed. *Sustainability* **2022**, *14*, 14827. [CrossRef]
31. Shaopan, X.; Zhaoliang, S.; Lukas, V.Z.; Laodong, G.; Changxun, Y.; Weiqi, W.; Qiang, L.; Hartley, P.I.; Yuanhe, Y.; Hongyan, L.; et al. Storage, patterns and influencing factors for soil organic carbon in coastal wetlands of China. *Glob. Change Biol.* **2022**, *28*, 6065–6085. [CrossRef]
32. Song, P.; Kim, G.; Mayer, A.; He, R.; Tian, G. Assessing the Ecosystem Services of Various Types of Urban Green Spaces Based on i-Tree Eco. *Sustainability* **2020**, *12*, 1630. [CrossRef]
33. Sun, Q.; Wang, P.; Zhou, H.M.; Wang, X.J.; Xie, W.Y.; Yang, Z.X. Spatial variability of soil carbon, nitrogen and phosphorus ecological stoichiometric characteristics in small watersheds in loess hilly area. *Chin. J. Ecol.* **2020**, *39*, 766–774. [CrossRef]
34. Wang, J.; Yang, R.; Bai, Z. Spatial variability and sampling optimization of soil organic carbon and total nitrogen for Minesoils of the Loess Plateau using geostatistics. *Ecol. Eng.* **2015**, *82*, 159–164. [CrossRef]
35. Wang, X.; Wang, C.; Zhang, Y.; Yan, Y. Pathway to identify and assess regional potential soil pollution risk from industrial activities: Case of Pearl River Delta region, China. *Int. J. Sustain. Dev. World Ecol.* **2025**, *32*, 511–524. [CrossRef]
36. Wu, L.; Li, L.; Yao, Y.; Qin, F.; Guo, Y.; Gao, Y.; Zhang, M. Spatial distribution of soil organic carbon and its influencing factors at different soil depths in a semiarid region of China. *Environ. Earth Sci.* **2017**, *76*, 654. [CrossRef]
37. Xin, Z.; Qin, Y.; Yu, X. Spatial variability in soil organic carbon and its influencing factors in a hilly watershed of the Loess Plateau, China. *Environ. Earth Sci.* **2016**, *137*, 660–669. [CrossRef]
38. Xing, H.; Yang, L. Retention of fragmented fine woody debris enhances soil health, microbial activity, and ecosystem functions in urban forests of Northeast China. *Plant Soil* **2025**, 1–19. [CrossRef]
39. Xiong, X.; Xiong, H.Q.; Guo, X.; Han, Y.; Qing, Z.; Chen, L.; Yu, H.M. Spatial variation characteristics of total nitrogen, organic carbon and carbon-to-nitrogen ratio of cultivated land in typical hilly areas in southern China and their influencing factors. *J. Plant Nutr. Fertil.* **2020**, *26*, 1656–1668.
40. Xiong, Z.; Li, S.; Yao, L.; Liu, G.; Zhang, Q.; Liu, W. Topography and land use effects on spatial variability of soil denitrification and related soil properties in riparian wetlands. *Ecol. Eng.* **2015**, *83*, 437–443. [CrossRef]
41. Chao, Y.; Huizeng, L.; Qingquan, L.; Aihong, C.; Rongling, X.; Tiezhu, S.; Jie, Z.; Wenxiu, G.; Xiang, Z.; Guofeng, W. Rapid Urbanization Induced Extensive Forest Loss to Urban Land in the Guangdong-Hong Kong-Macao Greater Bay Area, China. *Chin. Geogr. Sci.* **2021**, *31*, 93–108. [CrossRef]
42. Zhang, D.; Feng, Y.; Zhang, B.; Fan, X.; Han, Z.; Zhang, J. Unveiling the Spatial Variability of Soil Nutrients in Typical Karst Rocky Desertification Areas. *Water* **2024**, *16*, 334. [CrossRef]
43. Zhou, X.Y.; Wang, S.Q. The spatio-temporal response of ecosystem service value of the Yangtze River Economic Belt to urban expansion based on the GTWR model. *Res. Soil Water Conserv.* **2021**, *28*, 300–307. [CrossRef]
44. Zhu, Y.; Jia, P.; Liu, Y. Spatiotemporal evolution effects of habitat quality with the conservation policies in the Upper Yangtze River, China. *Sci. Rep.* **2025**, *15*, 5972. [CrossRef] [PubMed]

Disclaimer/Publisher's Note: The statements, opinions and data contained in all publications are solely those of the individual author(s) and contributor(s) and not of MDPI and/or the editor(s). MDPI and/or the editor(s) disclaim responsibility for any injury to people or property resulting from any ideas, methods, instructions or products referred to in the content.